DE GRUYTER OPEN

Int. J. of Applied Mechanics and Engineering, 2014, vol.19, No.4, pp.709-724
DOI: 10.2478/ijame-2014-0049

FINITE DIFFERENCE SOLUTION OF UNSTEADY FLOW PAST AN OSCILLATING SEMI-INFINITE VERTICAL PLATE WITH VARIABLE SURFACE TEMPERATURE AND UNIFORM MASS FLUX

R. MUTHUCUMARASWAMY* and B. SARAVANAN
Department of Applied Mathematics
Sri Venkateswara College of Engineering
Sriperumbudur, INDIA
E-mail: msamy@svce.ac.in

A finite difference solution of an unsteady flow past an oscillating semi-infinite vertical place with variable temperature and uniform mass flux is presented here. The fluid considered here is a gray, absorbing-emitting radiation but a non-scattering medium. The dimensionless governing equations are solved by an efficient, more accurate, and unconditionally stable and fast converging implicit scheme. The steady state velocity, temperature and concentration profiles are shown graphically. The effect of velocity and temperature for different physical parameters such as the thermal radiation, Schmidt number, thermal Grashof number and mass Grashof number is studied. It is observed that the velocity decreases in the presence of thermal radiation. It is also observed that the time taken to reach a steady-state is more in the case of vertical plate than horizontal plate.

Key words: radiation, vertical plate, finite-difference, variable temperature, uniform mass flux.

1. Introduction

Radiative heat and mass transfer play an important role in manufacturing industries for the design of reliable equipment. Nuclear power plants, gas turbines and various propulsion devices for aircraft, missiles, satellites and space vehicles are examples of such engineering applications. Radiative convective flows are encountered in countless industrial and environment processes e.g., heating and cooling chambers, fossil fuel combustion energy processes, evaporation from large open water reservoirs, astrophysical flows, solar power technology and space vehicle re-entry.

Cess (1966) studied the interaction of thermal radiation with free convection heat transfer . Soundalgekar and Takhar (1993) considered the radiative free convective flow of an optically thin gray-gas past a semi-infinite vertical plate. Radiation effects on a free convection flow past a semi-infinite vertical plate with mass transfer were studied by Chamkha *et al*. (2001). In all above studies, the stationary vertical plate is considered. Raptis and Perdikis (1999) studied the effects of thermal radiation and a free convection flow past a moving infinite vertical plate. Again, Raptis and Perdikis (2003) studied thermal radiation effects on a moving infinite vertical plate in the presence of mass diffusion. Radiation effects on a moving infinite vertical plate with variable temperature were studied by Muthucumaraswamy and Ganesan (2003). The boundary layer in thermal radiation absorbing and emitting media was studied by Viskanta and Grosh (1962).

* To whom correspondence should be addressed

The flow of a viscous, incompressible fluid past an infinite isothermal vertical plate, oscillating in its own plane, was solved by Soundalgekar (1979). The effect on the flow past a vertical oscillating plate due to a combination of concentration and temperature differences was studied extensively by Soundalgekar and Akolkar (1983). The effect of mass transfer on the flow past an infinite vertical oscillating plate in the presence of constant heat flux was studied by Soundalgekar *et al*. (1994). The effect of thermal radiation on the laminar free convection from a heated vertical plate wase studied by Arpaci (1968). An unstaedy flow of an incompressible viscous fluid past an impulsively started semi-infinite vertical plate with mass flux was studied by Muthucumaraswamy and Ganesan (1998).

However, the problem of an unsteady natural convection flow past an oscillating semi-infinite vertical plate with variable temperature and uniform mass flux has not received attention of any researcher. Hence it is proposed to study the flow of viscous incompressible fluid past an oscillating semi-infinite vertical plate with variable surface temperature and uniform mass flux by an implicit finite-difference scheme of Crank-Nicolson type. This study is found useful in distribution of cooling in a closed environment.

2. Mathematical formulation

A transient, laminar, unsteady natural convection flow of a viscous incompressible fluid past an oscillating semi-infinite isothermal vertical plate in the presence of thermal radiation has been considered. It is assumed that the concentration C' of the diffusing species in the binary mixture is very small in comparison to the other chemical species which are present. Here, the *x*-axis is taken along the plate in the vertically upward direction and the *y*-axis is taken normal to the plate. The physical model of the problem is shown in Fig.1. Initially, it is assumed that the plate and the fluid are of the same temperature and concentration. At time $t' > 0$, the plate starts oscillating in its own plane with frequency ω' against the gravitational field. The temperature of the plate is raised to $T_w(x)\left(= T_\infty + ax^n\right)$ and the concentration level near the plate is raised at a constant rate. The fluid considered here is a gray, absorbing-emitting radiation but a non-scattering medium and the viscous dissipation is assumed to be negligible. Then under the above assumptions, the governing boundary layer equations of mass, momentum and concentration for free the convective flow with usual Boussinesq's approximation are as follows

$$\frac{\partial u}{\partial x} + \frac{\partial v}{\partial y} = 0, \tag{2.1}$$

$$\frac{\partial u}{\partial t'} + u\frac{\partial u}{\partial x} + v\frac{\partial u}{\partial y} = g\beta\left(T - T_\infty\right) + g\beta^*\left(C' - C'_\infty\right) + \nu\frac{\partial^2 u}{\partial y^2}, \tag{2.2}$$

$$\rho C_p\left(\frac{\partial T'}{\partial t'} + u\frac{\partial T'}{\partial x} + v\frac{\partial T'}{\partial y}\right) = \frac{\partial^2 T'}{\partial y^2} - \frac{\partial q_r}{\partial y}, \tag{2.3}$$

$$\frac{\partial C'}{\partial t'} + u\frac{\partial C'}{\partial x} + v\frac{\partial C'}{\partial y} = D\frac{\partial^2 C'}{\partial y^2}. \tag{2.4}$$

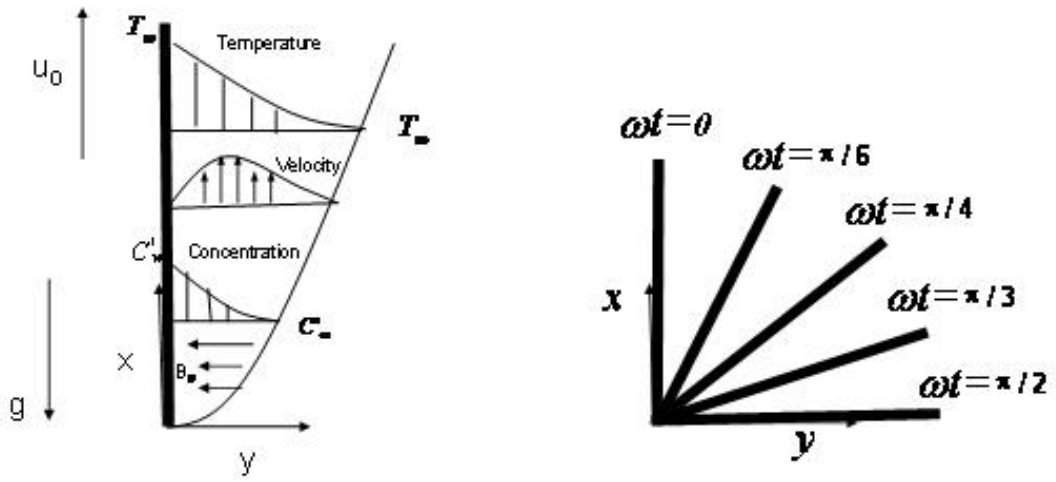

Fig.1. Physical model of the problem.

The initial and boundary conditions are

$$\begin{aligned}
&t' \le 0: \quad u = 0, && v = 0, && T' = T_\infty, && C' = C'_\infty, && \\
&t' > 0: \quad u = u_0 \cos \omega' t', && v = 0, && T' = T_\infty + a x^n, && \frac{\partial C'}{\partial y} = -\frac{j''}{D} \quad \text{at} && y = 0, \\
&\qquad\quad u = 0, && && T' = T_\infty, && C' = C'_\infty \quad \text{at} && x = 0, \\
&\qquad\quad u \to 0, && && T \to T_\infty, && C' \to C'_\infty \quad \text{as} && y \to \infty.
\end{aligned} \tag{2.5}$$

In the case of an optically thin gray gas the local radiant absorption is expressed by

$$\frac{\partial q_r}{\partial y} = -4a^* \sigma \left(T_\infty^4 - T'^4 \right). \tag{2.6}$$

We assume that the temperature differences within the flow are sufficiently small such that T^4 may be expressed as a linear function of the temperature. This is accomplished by expanding T^4 in a Taylor series about T_∞ and neglecting higher-order terms, thus

$$T'^4 \cong 4T_\infty^3 T' - 3T_\infty^4. \tag{2.7}$$

By using Eqs (2.6) and (2.7), Eq.(2.3) reduces to

$$\rho C_p \left(\frac{\partial T'}{\partial t'} + u \frac{\partial T'}{\partial x} + v \frac{\partial T'}{\partial y} \right) = k \frac{\partial^2 T'}{\partial y^2} + 16 a^* \sigma T_\infty^3 \left(T_\infty - T' \right). \tag{2.8}$$

On introducing the following non-dimensional quantities

$$U=\frac{u}{u_0},\qquad V=\frac{v\sqrt{L}}{\sqrt{u_0\nu}},\qquad t=\frac{t'u_0}{L},\qquad X=\frac{x}{L},\qquad Y=\frac{y\sqrt{u_0}}{\sqrt{L\nu}},\qquad T=\frac{T'-T_\infty}{T_w(L)-T_\infty},$$

$$\mathrm{Gr}=\frac{Lg\beta\left(T_w(L)-T_\infty\right)}{u_0^2},\qquad C=\frac{C'-C'_\infty}{\left(\frac{j''\sqrt{L\nu}}{D\sqrt{u_0}}\right)},\qquad \mathrm{Gc}=\frac{Lg\beta^*\left(\frac{j''\sqrt{L\nu}}{D\sqrt{u_0}}\right)}{u_0^2},\tag{2.9}$$

$$\omega'=\frac{\omega u_0}{L},\qquad R=\frac{16a^*L\nu\sigma T_\infty^3}{\alpha u_0},\qquad \mathrm{Pr}=\frac{\nu}{\alpha},\qquad \mathrm{Sc}=\frac{\nu}{D}.$$

Equations (2.1) to (2.4) are reduced to the following non-dimensional form

$$\frac{\partial U}{\partial X}+\frac{\partial V}{\partial Y}=0,\tag{2.10}$$

$$\frac{\partial U}{\partial t}+U\frac{\partial U}{\partial X}+V\frac{\partial U}{\partial Y}=\mathrm{Gr}\,T+\mathrm{Gc}\,C+\frac{\partial^2 U}{\partial Y^2},\tag{2.11}$$

$$\frac{\partial T}{\partial t}+U\frac{\partial T}{\partial X}+V\frac{\partial T}{\partial Y}=\frac{1}{\mathrm{Pr}}\frac{\partial^2 T}{\partial Y^2}-\frac{R}{\mathrm{Pr}}T,\tag{2.12}$$

$$\frac{\partial C}{\partial t}+U\frac{\partial C}{\partial X}+V\frac{\partial C}{\partial Y}=\frac{1}{\mathrm{Sc}}\frac{\partial^2 C}{\partial Y^2}.\tag{2.13}$$

The corresponding initial and boundary conditions in non-dimensional quantities are

$$t\le 0:\quad U=0,\quad V=0,\quad T=0,\quad C=0,$$

$$t>0:\ U=\cos\omega t,\quad V=0,\quad T=X^n,\quad \frac{\partial C}{\partial Y}=-1\quad \text{at}\quad Y=0,\tag{2.14}$$

$$U=0,\quad T=0,\quad C=0\quad \text{at}\quad X=0,$$

$$U\to 0,\quad T\to 0,\quad C\to 0\quad \text{as}\quad Y\to\infty.$$

3. Numerical technique

In order to solve the unsteady, non-linear coupled Eqs (2.10) to (2.13) under the conditions of Eq.(2.14), an implicit finite difference scheme of Crank- Nicolson type has been employed. The finite difference equations corresponding to Eqs (2.10) to (2.13) are as follows

$$\frac{\left[U_{i,j}^{n+1}-U_{i-1,j}^{n+1}+U_{i,j}^{n}-U_{i-1,j}^{n}+U_{i,j-1}^{n+1}-U_{i-1,j-1}^{n+1}+U_{i,j-1}^{n}-U_{i-1,j-1}^{n}\right]}{4\Delta X}+$$
$$+\frac{\left[V_{i,j}^{n+1}-V_{i,j-1}^{n+1}+V_{i,j}^{n}-V_{i,j-1}^{n}\right]}{2\Delta Y}=0, \tag{3.1}$$

$$\frac{\left[U_{i,j}^{n+1}-U_{i,j}^{n}\right]}{\Delta t}+U_{i,j}^{n}\frac{\left[U_{i,j}^{n+1}-U_{i-1,j}^{n+1}+U_{i,j}^{n}-U_{i-1,j}^{n}\right]}{2\Delta X}+$$
$$+V_{i,j}^{n}\frac{\left[U_{i,j+1}^{n+1}-U_{i,j-1}^{n+1}+U_{i,j+1}^{n}-U_{i,j-1}^{n}\right]}{4\Delta Y}=\frac{\mathrm{Gr}}{2}\left[T_{i,j}^{n+1}+T_{i,j}^{n}\right]+\frac{\mathrm{Gc}}{2}\left[C_{i,j}^{n+1}+C_{i,j}^{n}\right]+ \tag{3.2}$$
$$+\frac{\left[U_{i,j-1}^{n+1}-2U_{i,j}^{n+1}+U_{i,j+1}^{n+1}+U_{i,j-1}^{n}-2U_{i,j}^{n}+U_{i,j+1}^{n}\right]}{2\left(\Delta Y\right)^{2}},$$

$$\frac{\left[T_{i,j}^{n+1}-T_{i,j}^{n}\right]}{\Delta t}+U_{i,j}^{n}\frac{\left[T_{i,j}^{n+1}-T_{i-1,j}^{n+1}+T_{i,j}^{n}-T_{i-1,j}^{n}\right]}{2\Delta X}+$$
$$+V_{i,j}^{n}\frac{\left[T_{i,j+1}^{n+1}-T_{i,j-1}^{n+1}+T_{i,j+1}^{n}-T_{i,j-1}^{n}\right]}{4\Delta Y}= \tag{3.3}$$
$$=\frac{1}{\mathrm{Pr}}\frac{\left[T_{i,j-1}^{n+1}-2T_{i,j}^{n+1}+T_{i,j+1}^{n+1}+T_{i,j-1}^{n}-2T_{i,j}^{n}+T_{i,j+1}^{n}\right]}{2\left(\Delta Y\right)^{2}}-\frac{R\left(T_{i,j}^{n+1}+T_{i,j}^{n}\right)}{2\mathrm{Pr}},$$

$$\frac{\left[C_{i,j}^{n+1}-C_{i,j}^{n}\right]}{\Delta t}+U_{i,j}^{n}\frac{\left[C_{i,j}^{n+1}-C_{i-1,j}^{n+1}+C_{i,j}^{n}-C_{i-1,j}^{n}\right]}{2\Delta X}+$$
$$+V_{i,j}^{n}\frac{\left[C_{i,j+1}^{n+1}-C_{i,j-1}^{n+1}+C_{i,j+1}^{n}-C_{i,j-1}^{n}\right]}{4\Delta Y}= \tag{3.4}$$
$$=\frac{1}{\mathrm{Sc}}\frac{\left[C_{i,j-1}^{n+1}-2C_{i,j}^{n+1}+C_{i,j+1}^{n+1}+C_{i,j-1}^{n}-2C_{i,j}^{n}+C_{i,j+1}^{n}\right]}{2\left(\Delta Y\right)^{2}}.$$

The concentration boundary condition at $Y=0$ in the finite difference form is

$$\frac{1}{2}\frac{\left[C_{i,1}^{n+1}+C_{i,1}^{n}-C_{i,-1}^{n+1}-C_{i,-1}^{n}\right]}{2\Delta Y}=-1. \tag{3.5}$$

At $Y=0$ (i.e., $j=0$), Eq.(3.4) becomes

$$\frac{\left[C_{i,0}^{n+1}-C_{i,0}^{n}\right]}{\Delta t}+U_{i,0}^{n}\frac{\left[C_{i,0}^{n+1}-C_{i-1,0}^{n+1}+C_{i,0}^{n}-C_{i-1,0}^{n}\right]}{2\,\Delta X}=$$
$$=\frac{1}{\mathrm{Sc}}\frac{\left[C_{i,-1}^{n+1}-2C_{i,0}^{n+1}+C_{i,1}^{n+1}+C_{i,-1}^{n}-2C_{i,0}^{n}+C_{i,1}^{n}\right]}{2\left(\Delta Y\right)^{2}}. \tag{3.6}$$

After eliminating $C_{i,-1}^{n+1}+C_{i,-1}^{n}$ using Eq.(3.5), Eq.(3.6) reduces to the form

$$\frac{\left[C_{i,0}^{n+1}-C_{i,0}^{n}\right]}{\Delta t}+U_{i,0}^{n}\frac{\left[C_{i,0}^{n+1}-C_{i-1,0}^{n+1}+C_{i,0}^{n}-C_{i-1,0}^{n}\right]}{2\,\Delta X}=$$
$$=\frac{1}{\mathrm{Sc}}\frac{\left[C_{i,1}^{n+1}-C_{i,0}^{n+1}+C_{i,1}^{n}-C_{i,0}^{n}+2\Delta Y\right]}{\left(\Delta Y\right)^{2}}. \tag{3.7}$$

Here the region of integration is considered as a rectangle with sides X_{max} (= *1*) and Y_{max} (=*20*), where Y_{max} corresponds to $Y = \infty$ which lies very well outside both the momentum and energy boundary layers. The maximum of *Y* was chosen as 20 after some preliminary investigations so that the last two of the boundary conditions Eqs (2.14) are satisfied with in the tolerance limit 10^{-5}.

After experimenting with a few sets of mesh sizes they have been fixed at the level $\Delta X = 0.05$, $\Delta Y = 0.25$, with time step $\Delta t = 0.01$. In this case, the spatial mesh sizes are reduced by *50%* in one direction, and later in both directions, and the results are compared. It is observed that when the mesh size is reduced by *50%* in the *Y*-direction, the results differ in the fifth decimal place. While the mesh sizes are reduced by *50%* in *X*-direction or in both directions, the results are comparable to three decimal places. Hence, the above mesh sizes have been considered as appropriate for calculations. The coefficients $U_{i,j}^{n}$ and $V_{i,j}^{n}$ appearing in the finite difference equation are treated as constants at any one time step. Here *i*-designates the grid point along the *X* - direction, *j* along the *Y*- direction and *k* to the *t*-time. The values of *U, V* and *T* are known at all grid points at *t = 0* from the initial conditions.

The computations of *U, V, T* and *C* at time level (*n +1*) using the values at previous time level (*n*) are carried out as follows: the finite-difference Eqs (3.4) and (3.7) at every internal nodal point on a particular *i*-level constitute a tri-diagonal system of equations. The system of equations is solved by using The Thomas algorithm as discussed in Carnahan *et al*. (1969). Thus, the values of *C* are found at every nodal point for a particular *i* at $(n+1)^{th}$ time level. Similarly, the values of *T* are calculated from Eq.(3.3) .Using the values of *C* and *T* at $(n+1)^{th}$ time level in Eq.(3.2) , the values of *U* at $(n+1)^{th}$ time level are found in a similar manner. Thus, the values of *C, T* and *U* are known on a particular *i*-level. Finally, the values of *V* are calculated explicitly using Eq.(3.1) at every nodal point at particular *i*-level at $(n+1)^{th}$ time level. This process is repeated for various *i*-levels. Thus the values of *C, T, U* and *V* are known at all grid points in the rectangle region at $(n+1)^{th}$ time level.

Computations are carried out In a similar manner by moving along the *i*-direction. After computing the values corresponding to each *i* at *a* time level, the values at the next time level are determined in a similar manner. Computations are repeated until the steady-state is reached. The steady-state solution is assumed to have been reached, when the absolute difference between the values of *U*, and as well as temperature *T* and concentration *C* at two consecutive time steps are less than 10^{-5} at all grid points.

4. Discussion of results

The numerical values of the velocity, temperature and concentation are computed for different parameters such as the radiation parameter, Schmidt number, phase angle, thermal Grashof number and mass Grashof number. The purpose of the calculations given here is to assess the effects of the parameters $\omega t, R, \mathrm{Gr}, \mathrm{Gc}$ and Sc upon the nature of the flow and transport. The values of the Prandtl number Pr is chosen such that they represent air (Pr = *0.71*) and the Schmidt number Sc = *0.6* (water vapour).

The steady-state velocity profiles for different phase angles are shown in Fig.2. The velocity profiles presented are those at $X = 1.0$. It is observed that for different phase angles $(\omega t = 0, \pi/6, \pi/3, \pi/2)$, Gr=*5*=Gc and *R=2* the velocity decreases with increasing the phase angle. Here $\omega t = 0$ represents the vertical plate. Note that the velocity profile grows from $U = 1$ and $\omega t = \pi/2$ refers to the horizontal plate and the velocity profiles starting with $U = 0$. The numerical value satisfies the prescribed boundary conditions. It is also observed that the time taken to reach the steady-state is larger in the case of a vertical plate than a horizontal plate.

In Fig.3, the velocity profiles for different values of thermal Grashof number (Gr=*2*, *5*), mass Grashof number (Gc=*2*, *5*), $\omega t = \pi/6$ and *R=2* are shown graphically. This shows that the velocity increases with increasing the thermal Grashof number or mass Grashof number. As the thermal Grashof number or mass Grashof number increase, the buoyancy effect becomes more significant, as expected; it implies that, more fluid is entrained from the free stream due to the strong buoyancy effects. The effect of velocity for different radiation parameters (*R = 0.2*, *2*, *5*), $\omega t = \pi/6$ and Gr=Gc=*5* is shown in Fig.4. It is observed that the velocity increases with decreasing the radiation parameter. This shows that velocity decreases in the presence of high thermal radiation.

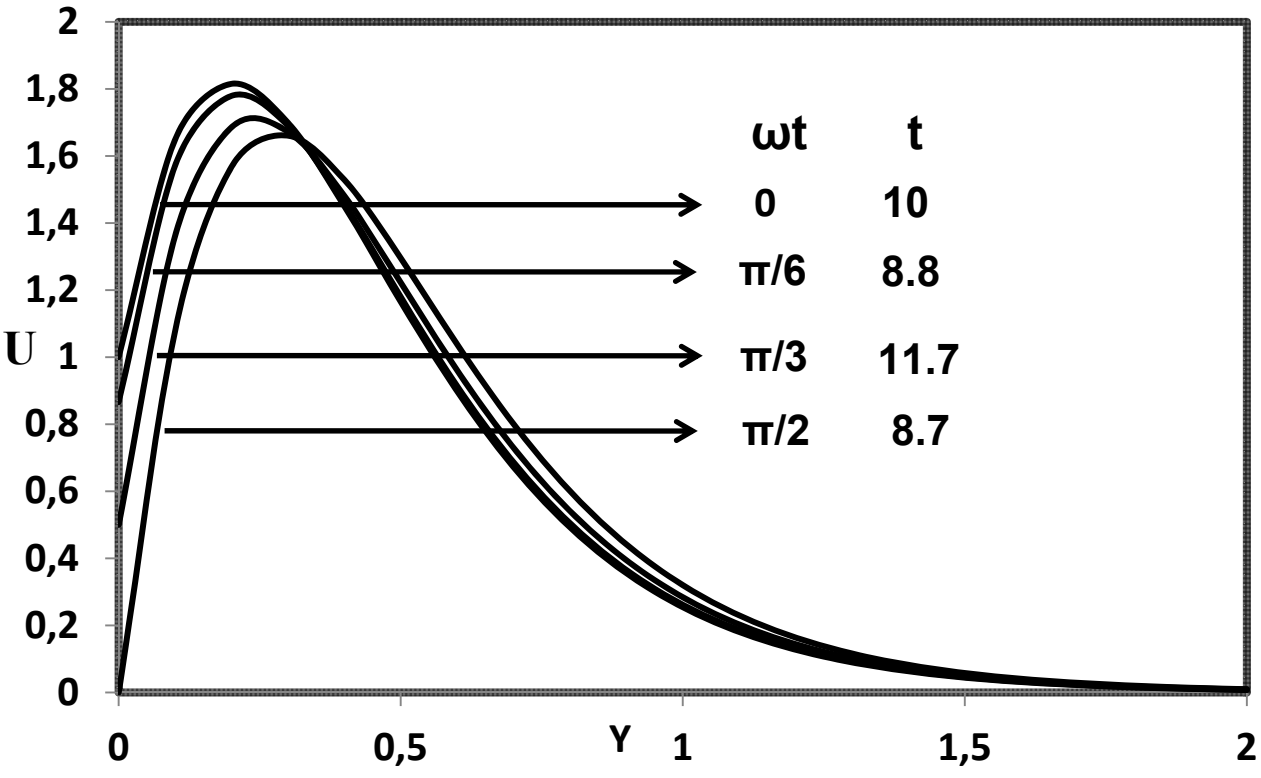

Fig.2. Steady state velocity profiles for different values of ωt.

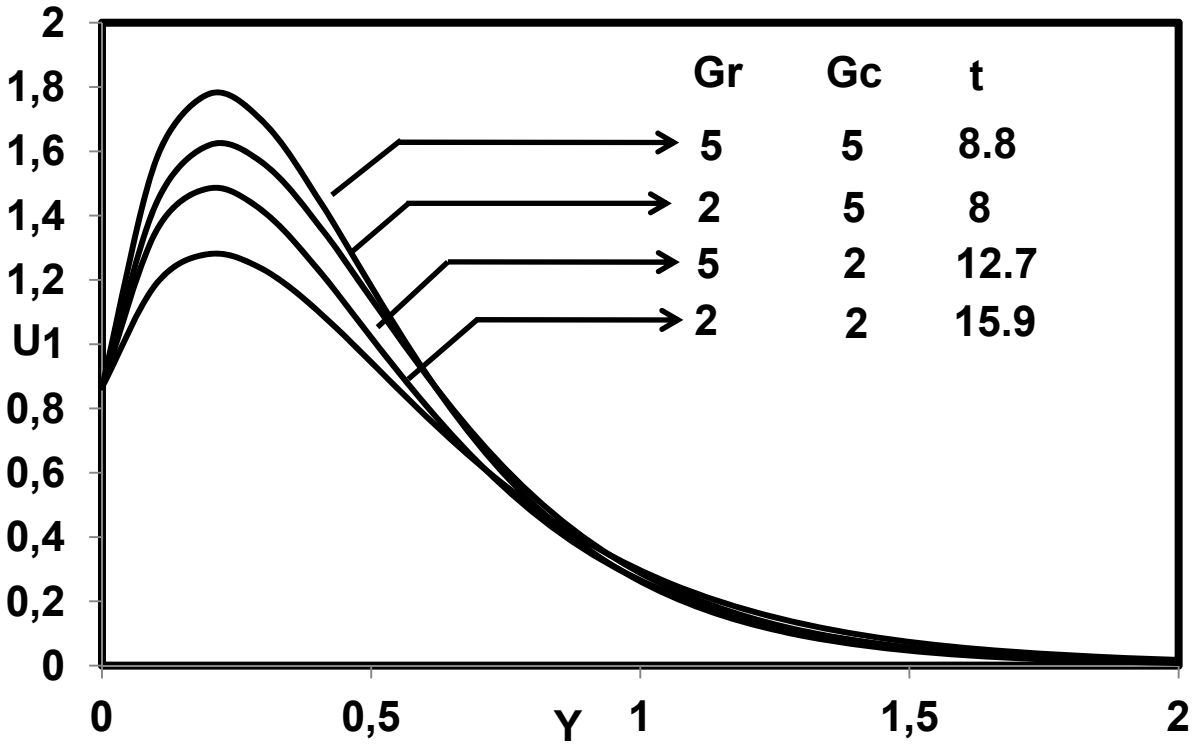

Fig.3. Steady state velocity profiles for different values of Gr and Gc.

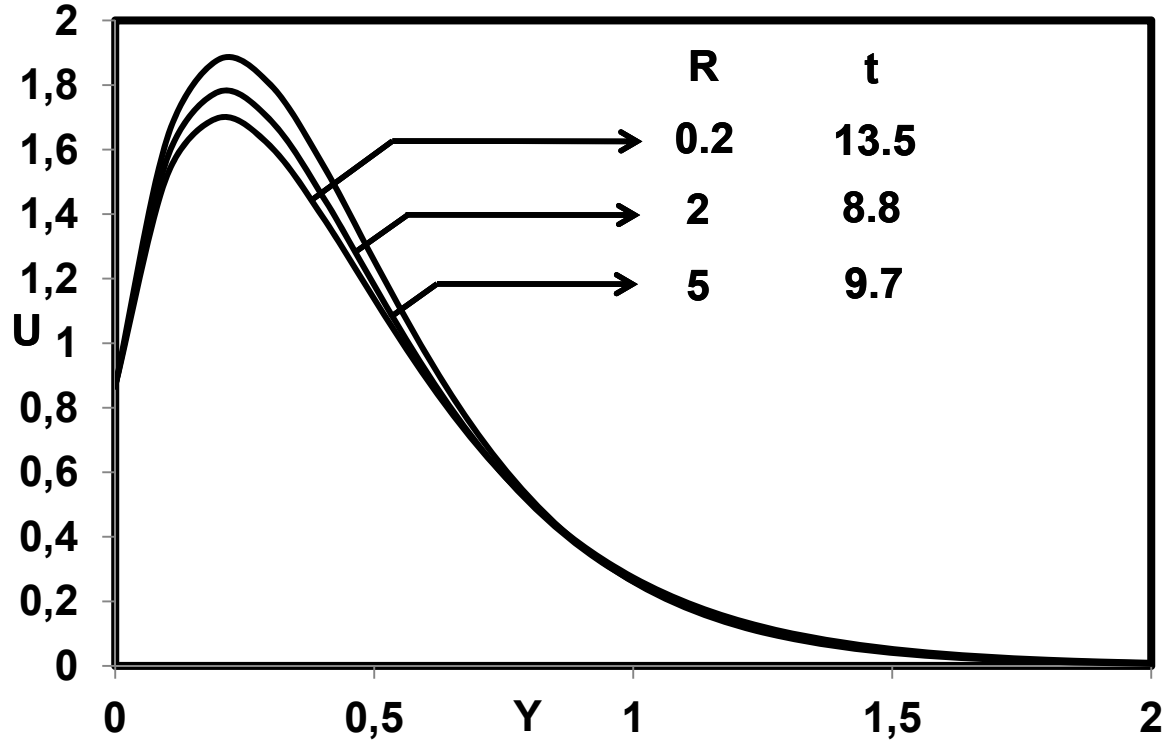

Fig.4. Steady state velocity profiles for different values of *R*.

The steady-state velocity profiles for different values of the Schmidt number (Sc=*0.16*, *0.3*, *0.6*, *2.01*), Gr=Gc=*5*, $\omega t = \pi / 6$ and *R=2* are shown in Fig.5. The velocity profiles presented are those at *X = 1.0*. It is observed that the velocity decreases with increasing the Schmidt number and the steady-state value increases with increasing the Schmidt number. The velocity boundary layer seems to grow in the direction of motion of the plate. It is observed that near the leading edge of a semi-infinite vertical plate moving in a fluid, the boundary layer develops along the direction of the plate. However, the time required for the velocity to reach the steady-state depends upon the Schmidt number. This shows that the contribution of mass diffusion to the buoyancy force increases the maximum velocity significantly.

The temperature profiles for different values of the thermal radiation parameter (*R=0.2*, *2*, *5*, *10*) are shown in Fig.6. It is observed that the temperature increases with decreasing *R*. This shows that the buoyancy effect on the temperature distribution is very significant in air (Pr = *0.71*). It is known that the radiation parameter and Prandtl number play an important role in flow phenomena because, it is a measure of the relative magnitude of the viscous boundary layer thickness to the thermal boundary layer thickness. The concentration profiles for different values of the Schmidt number (Sc=*0.16*, *0.3*, *0.6*, *2.01*) are shown in Fig.7. It is observed that the plate concentration increases with decreasing Sc.

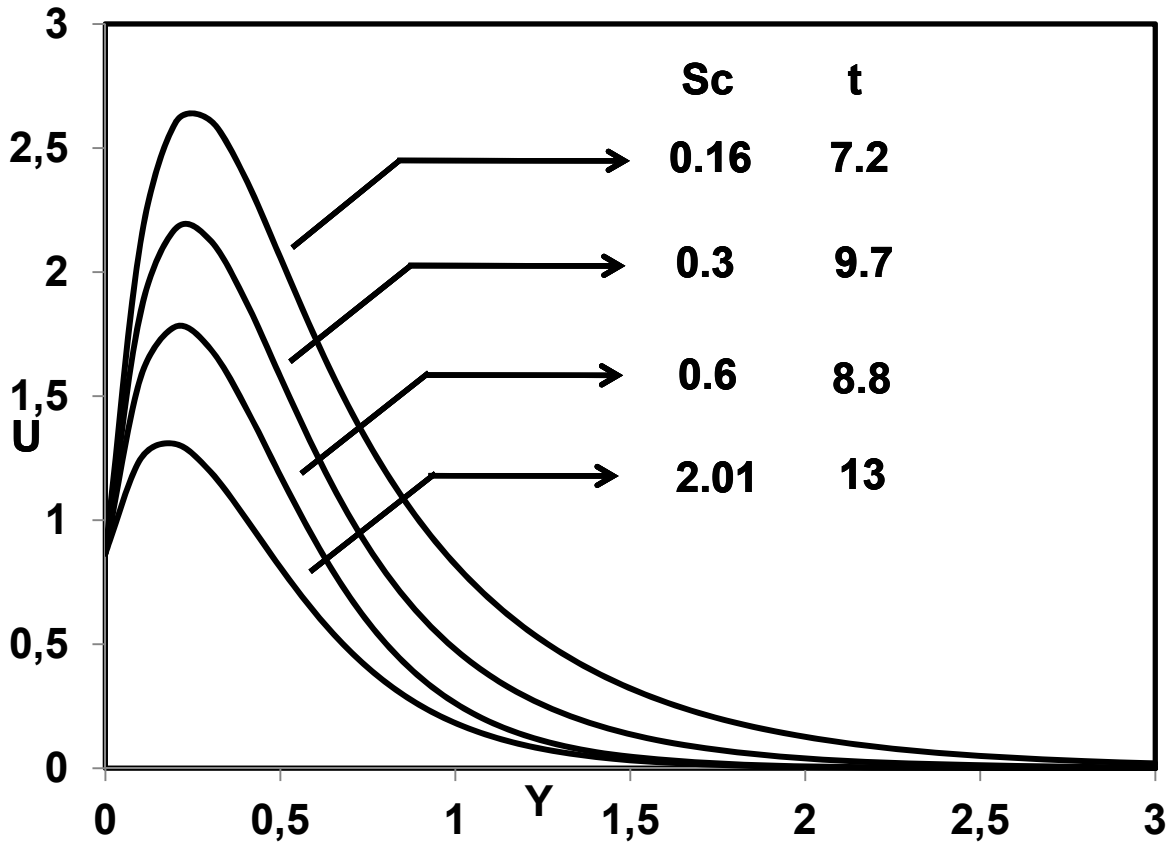

Fig.5. Steady state velocity profiles for different values of Sc.

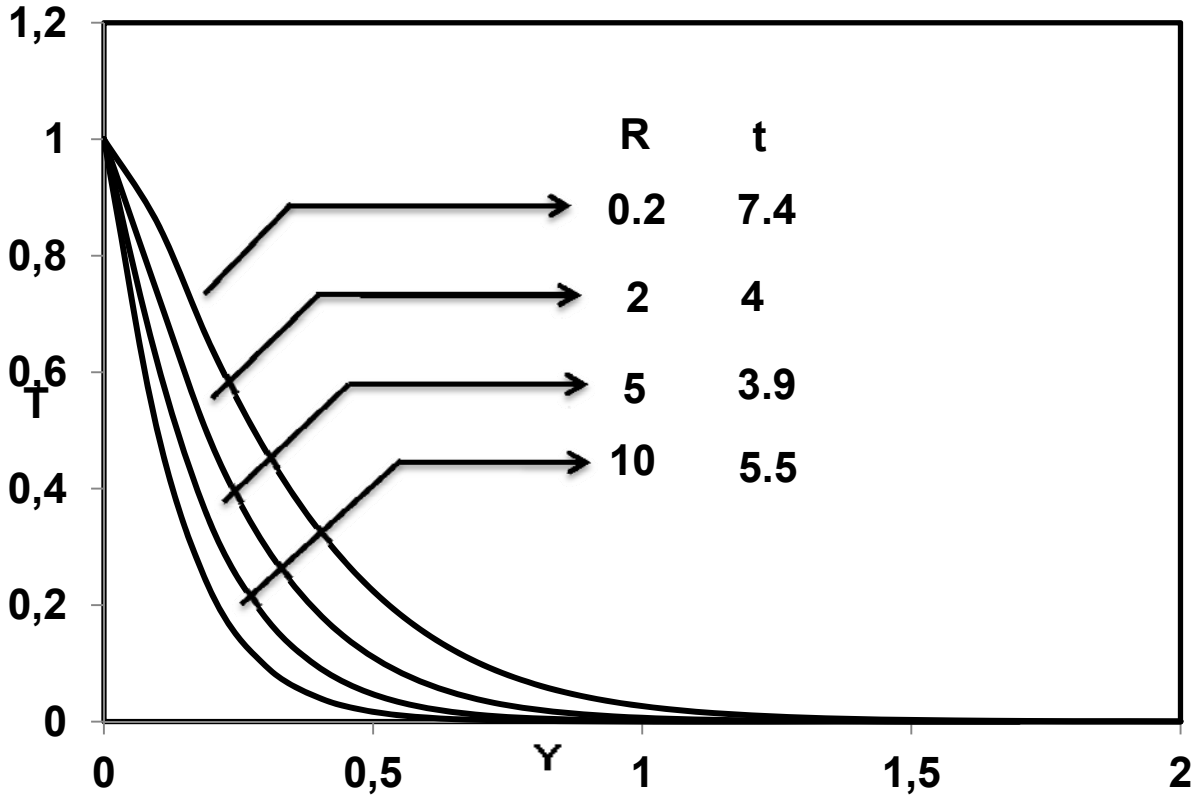

Fig.6. Temperature profiles for different values of *R*.

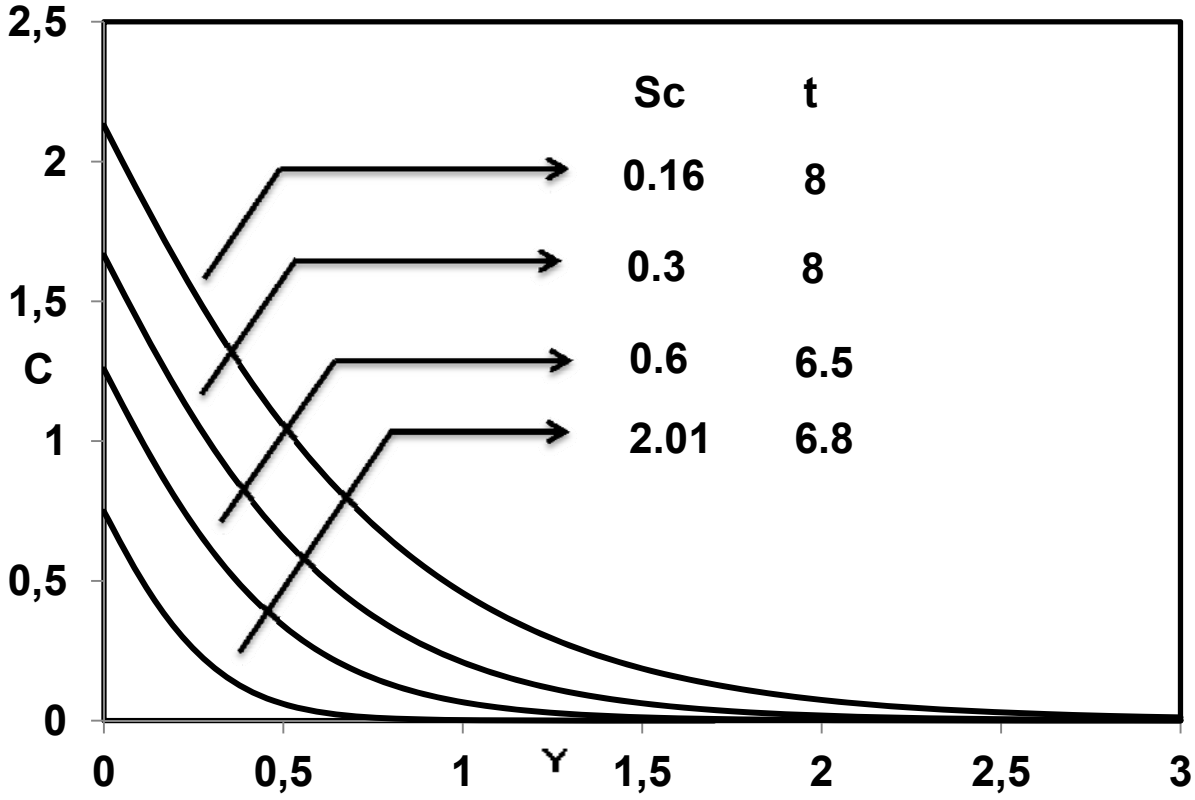

Fig.7. Concentration profiles for different values of Sc.

Knowing the velocity and temperature field, it is customary to study the skin-friction, Nusselt number and Sherwood number. The local as well as average values of the skin-friction, Nusselt number and Sherwood number in dimensionless form are as follows

$$\tau_X = -\left(\frac{\partial U}{\partial Y}\right)_{Y=0}, \tag{4.1}$$

$$\bar{\tau} = -\int_0^1 \left(\frac{\partial U}{\partial Y}\right)_{Y=0} dX, \tag{4.2}$$

$$\mathrm{Nu}_X = \frac{-X\left(\frac{\partial T}{\partial Y}\right)_{Y=0}}{T_{Y=0}}, \tag{4.3}$$

$$\overline{\mathrm{Nu}} = -\int_0^1 \left[\frac{\left(\frac{\partial T}{\partial Y}\right)_{Y=0}}{T_{Y=0}}\right] dX, \tag{4.4}$$

$$\mathrm{Sh}_X = -X\left(\frac{\partial C}{\partial Y}\right)_{Y=0}, \tag{4.5}$$

$$\overline{\mathrm{Sh}} = -\int_0^1 \left(\frac{\partial C}{\partial Y}\right)_{Y=0} dX. \tag{4.6}$$

The derivatives involved in Eqs (4.1) to (4.6) are evaluated using the five-point approximation formula and then the integrals are evaluated using the Newton-Cotes closed integration formula.

The local skin-friction, Nusselt number and Sherwood number are plotted in Figs 8, 9 and 10 respectively. Local skin-friction values for different phase angles are evaluated from Eq.(4.1) and plotted in Fig.8 as a function of the axial coordinate. The local wall shear stress increases with decreasing the phase angle. The trend shows that the wall shear stress is larger in the case of a vertical plate than a horizontal plate. The local Nusselt number for different values of the thermal radiation parameter is presented in Fig.9 as a function of the axial co-ordinate. The trend shows that the Nusselt number increases with increasing the values of the thermal radiation parameter. It is clear that the rate of heat transfer is larger in the presence of thermal radiation. The local Sherwood numbers for different values of the Schmidt number are shown in Fig.10. As expected, the rate of mass transfer increases with increasing values of the Schmidt number. This trend is just reversed as compared to the concentration field for different values of the Schmidt number given in Fig.7.

The average values of the skin-friction, Nusselt number and Sherwood number are shown in Figs 11, 12 and 13 respectively. The effects of the different phase angles on the average values of the skin-friction are shown in Fig.11. The average skin-friction decreases with decreasing or with increasing values of the phase angle. Figure 12 illustrates that the average Nusselt number increases with increasing the radiation parameter. From Fig.13, it is observed that the average Sherwood number increases with increasing values of the Schmidt number.

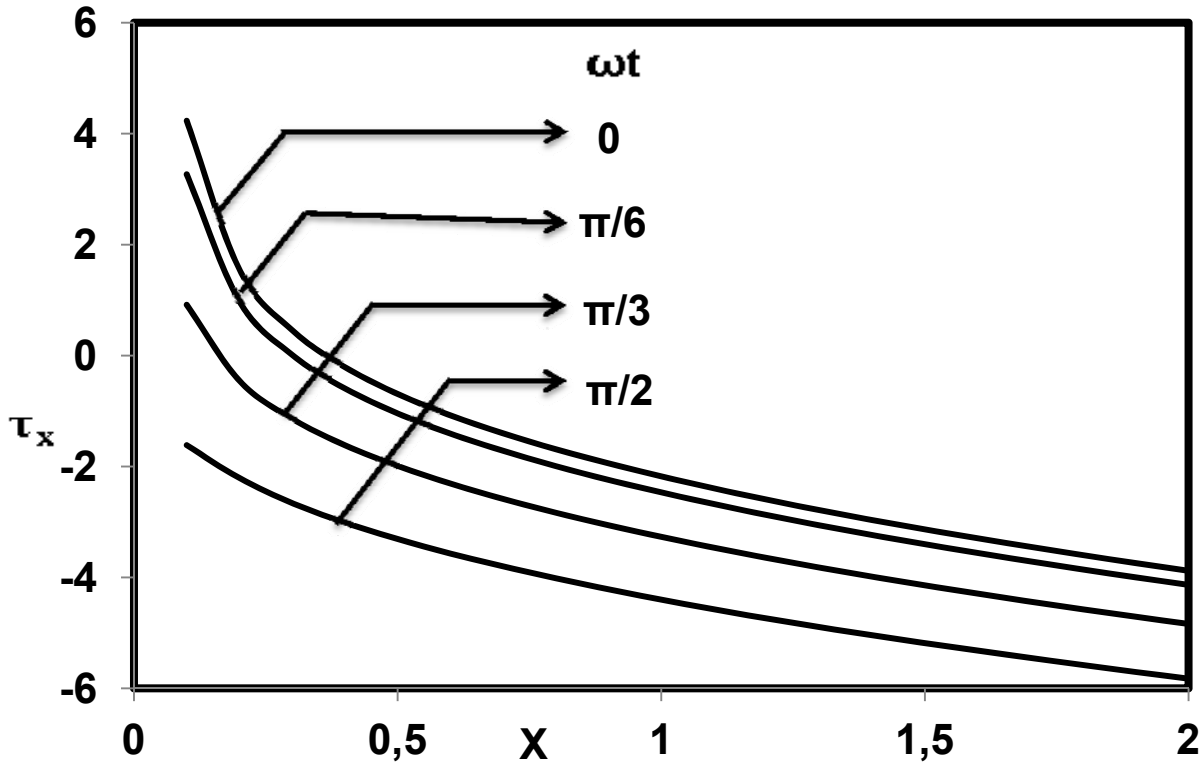

Fig.8. Local skin friction.

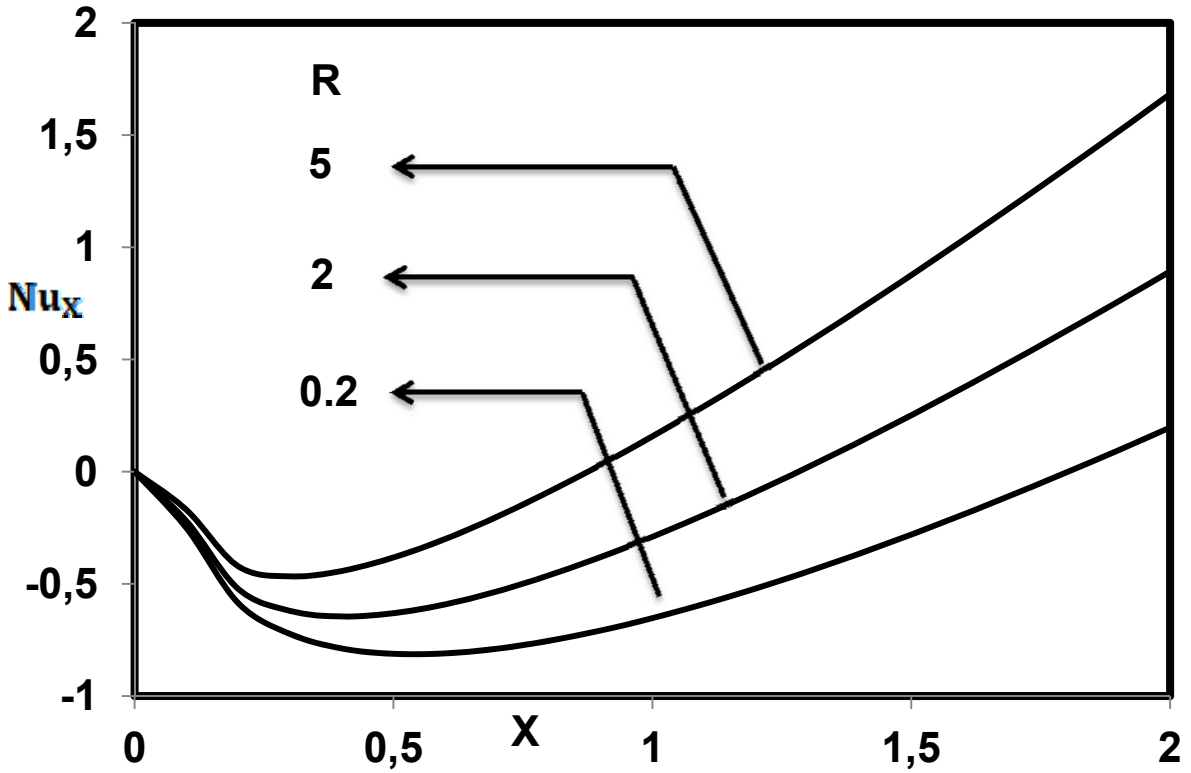

Fig.9. Local Nusselt number.

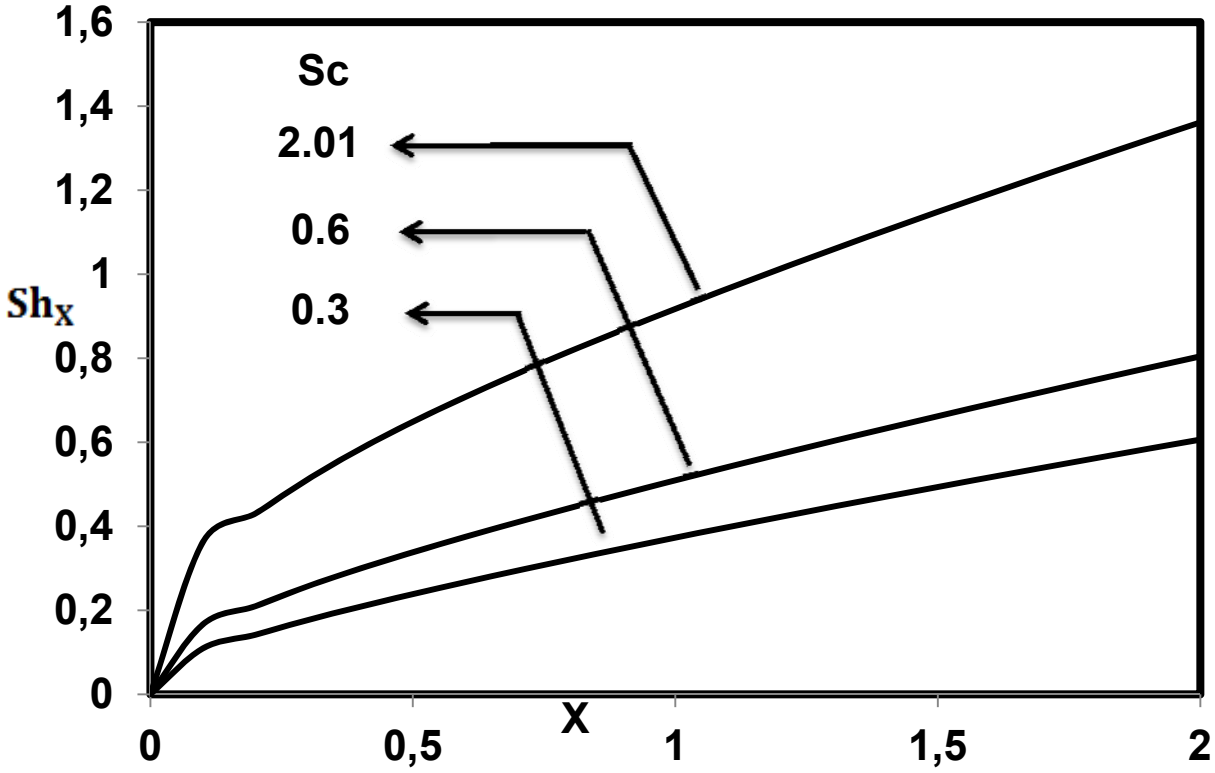

Fig.10. Local Sherwood number.

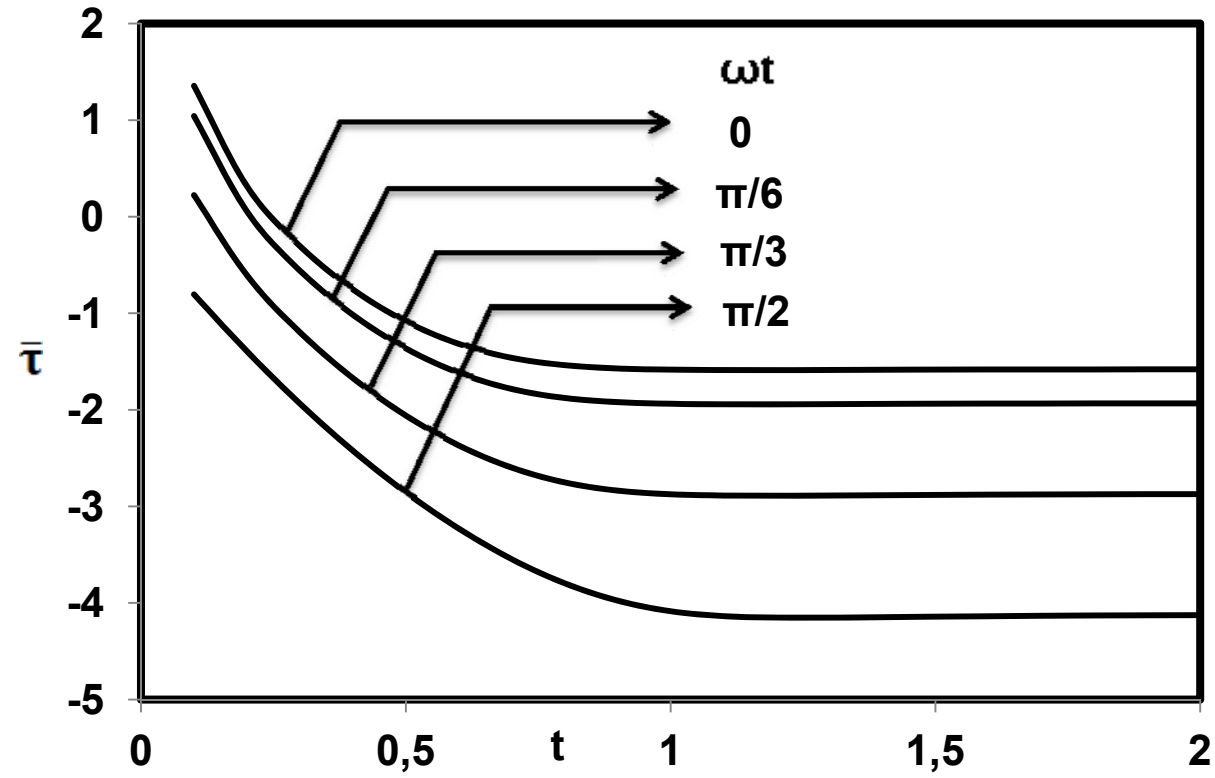

Fig.11. Average skin friction.

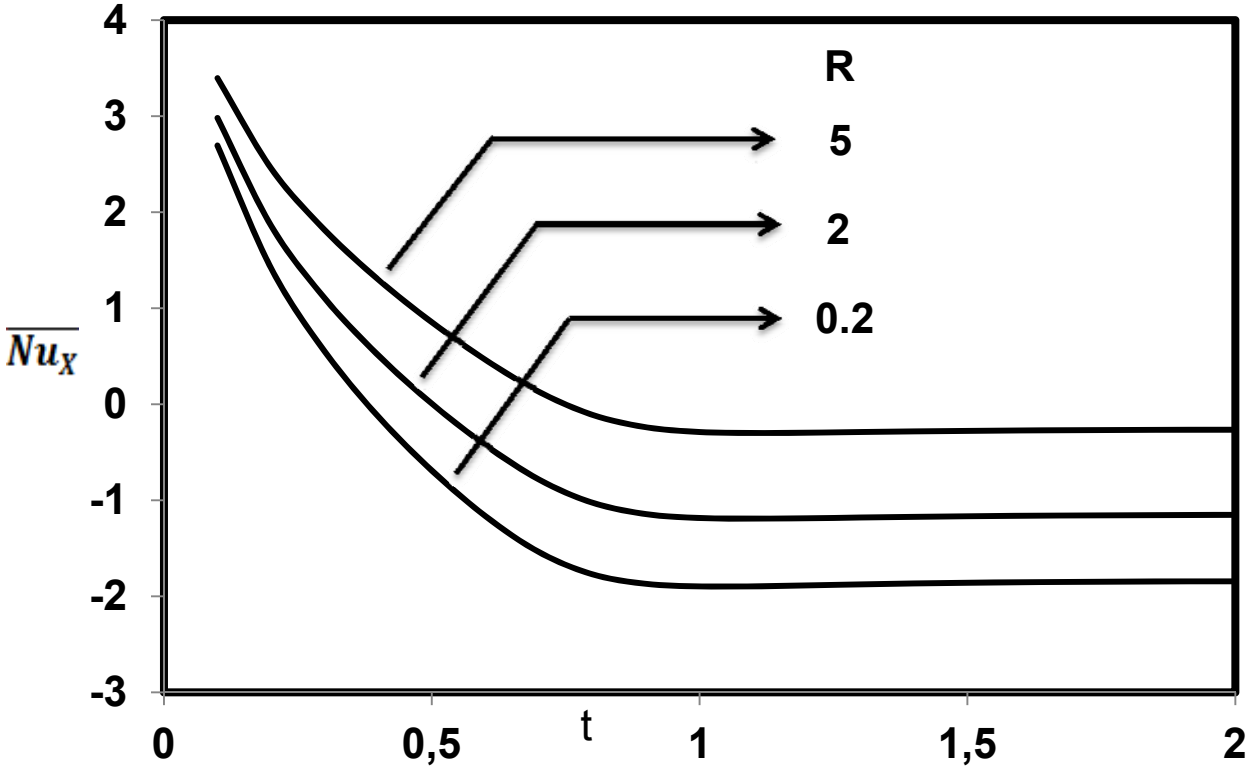

Fig.12. Average Nusselt number.

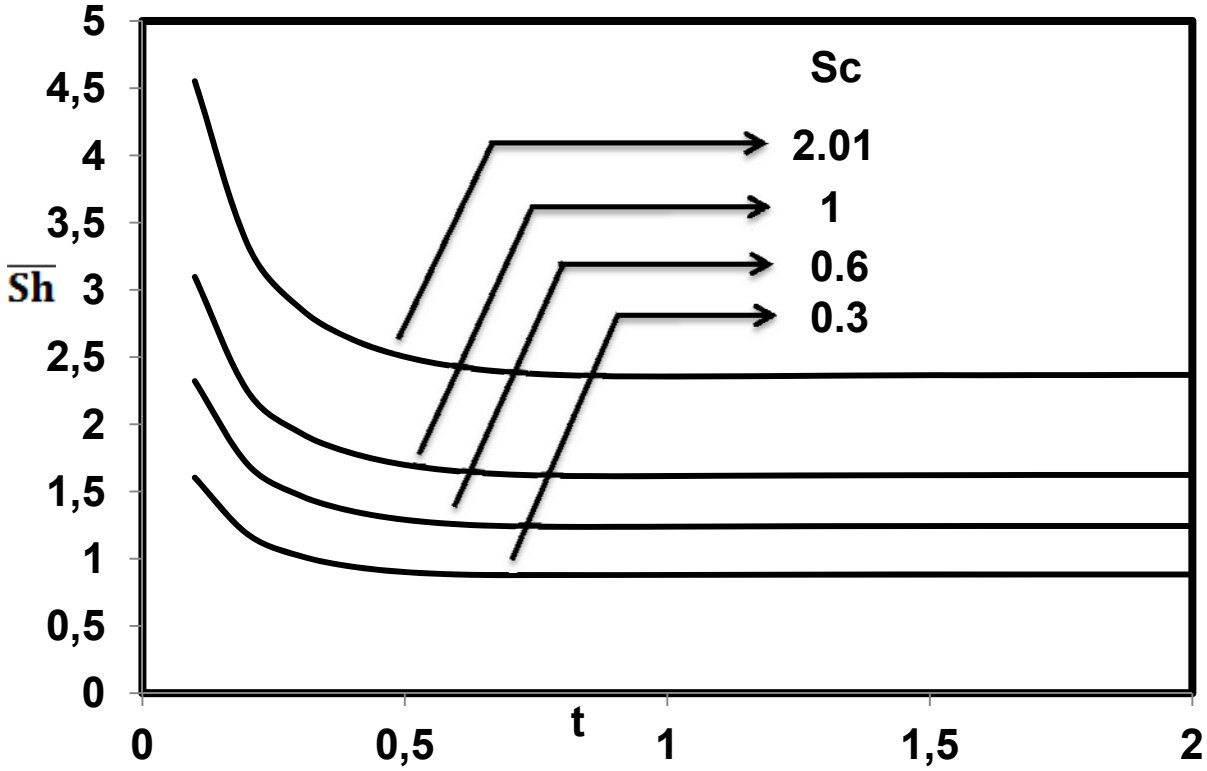

Fig.13. Average Sherwood number.

5. Conclusions

The finite difference solution of thermal radiation effects on an unsteady flow past an oscillating semi-infinite vertical plate with prescribed variable surface temperature and uniform mass flux has been studied. The dimensionless governing equations are solved by an implicit scheme of Crank-Nicolson type. The effects of velocity, temperature and concentration for different parameters are studied. The local as well as average skin-friction, Nusselt number and Sherwood number are shown graphically. The study shows that the number of time steps to reach the steady-state depends strongly on the radiation parameter. It is observed that the contribution of mass diffusion to the buoyancy force increases the maximum velocity significantly. The conclusions of the study are as follows:

(i) The velocity increases with decreasing the radiation parameter.
(ii) The steady-state velocity increases with decreasing the phase angle.
(ii) The time taken to reach steady-state is larger in the case of a vertical plate than a horizontal plate.

Nomenclature

a^* – absorbtion constants
C – dimensionless concentration
C' – species concentration in the fluid
C_p – specific heat at constant pressure
C'_w – concentration of the plate
C'_∞ – concentration in the fluid far away from the plate
D – mass diffusion coefficient
Gc – mass Grashof number
Gr – thermal Grashof number
g – acceleration due to gravity
k – thermal conductivity
M – magnetic field parameter
$\overline{\mathrm{Nu}}$ – dimensionless average Nusselt number
Nu_x – dimensionless local Nusselt number
Pr – Prandtl number
R – thermal radiation parameter
Sc – Schmidt number
$\overline{\mathrm{Sh}}$ – dimensionless average Sherwood number
Sh_x – dimensionless local Sherwood number
T – temperature of the fluid near the plate
T' – temperature
T'_w – temperature of the plate
T'_∞ – temperature of the fluid far away from the plate
t' – time
u_0 – velocity of the plate
u, v – velocity of the components of the fluid in X, Y- directions, respectively
w –conditions at the wall
X – dimensionless coordinate along the plate
x – coordinate along the plate
Y – dimensionless coordinate axis normal to the plate
y – coordinate axis normal to the plate
α – thermal diffusivity

β – volumetric coefficient of thermal expansion
β^* – volumetric coefficient of expansion with concentration
μ – coefficient of viscosity
θ –dimensionless temperature
ν – kinematic viscosity
ρ – density of the fluid
σ – electric conductivity
$\bar{\tau}$ – dimesionless average skin friction
τ_x – dimensionless local skin friction
ω – dimensional frequency of oscillation
ω' – frequency of oscillation
ωt – dimensional phase angle
$\omega' t'$ – phase angle
∞ – free stream conditions

References

Carnahan B., Luther H.A. and Wilkes J.O. (1969): *Applied Numerical Methods*. – New York : John Wiley and Sons.

Cess R.D. (1966): *The interaction of thermal radiation with free convection heat transfer.* – Int. J. Heat Mass Transfer, vol.9, pp.1269-1277.

Chamkha A.J., Takhar H.S. and Soundalgekar V.M. (2001): *Radiation effects on free convection flow past a semi-infinite vertical plate with mass transfer.* – Chemical Engineering Journal, vol.84, pp.335-342.

Muthucumaraswamy R. and Ganesan P. (1998): *Unsteady flow past an impulsively started isothermal vertical plate with mass flux.* – Journal of Energy, Heat and Mass Transfer, vol.20, pp.141-148.

Muthucumaraswamy R. and Ganesan P. (2003): *Radiation effects on flow past an impulsively started infinite vertical plate with variable temperature*. – Int. J. of Appl. Mech. and Engg., vol.8, pp.125-129.

Raptis A. and Perdikis C. (1999): *Radiation and free convection flow past a moving plate.* – Int. J. App. Mech. and Engg., vol.4, pp.817-821.

Raptis A. and Perdikis C. (2003): *Thermal radiation of an optically thin gray gas*. – Int. J. App. Mech. and Engg., vol.8, pp.131-134.

Soundalgekar V.M. (1979): *Free convection effects on the flow past a vertical oscillating plate.* – Astrophysics and Space Science, vol.64, pp.165-172.

Soundalgekar V.M. and Alolkar S.P. (1983): *Effects of free convection currents and mass transfer on the flow past a vertical oscillating plate*. – Astrophysics and Space Science, vol.89, pp.241-254.

Soundalgekar V.M., Lahurikar R.M., Pohanerkar S.G. and Birajdar N.S. (1994): *Effects of mass transfer on the flow past an oscillating infinite vertical plate with constant heat flux.* – Thermophysics and Aero Mech., vol.1, pp.119-124.

Soundalgekar V.M. and Takhar H.S. (1993): *Radiation effects on free convection flow past a sem-infinite vertical plate*. – Journal of Modeling, Measurements and Control, B51, pp.31-40.

Vedat S.A. (1968): *Effect of thermal radiation on the laminar free convection from a heated vertical plate.* – Int. J. Heat Mass Transfer, vol.11, pp.871-881.

Viskanta R. and Grosh R.J. (1962): *Boundary layer in thermal radiation absorbing and emitting media*. – Int. J. Heat Mass Transfer, vol.5, pp.795-806.

Received: August 9, 2013
Revised: May 23, 2014